https://doi.org/10.1093/plcell/koad190 THE PLANT CELL 2023: 1–15

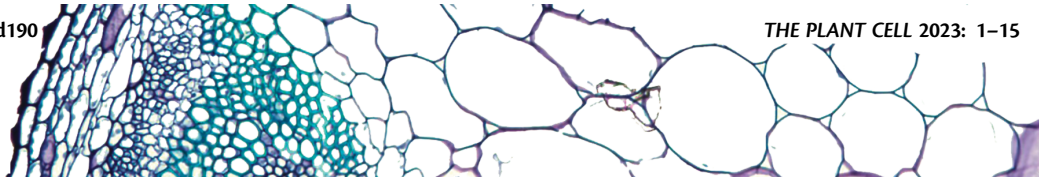

Research Article

# VERNALIZATION1 represses *FLOWERING PROMOTING FACTOR1-LIKE1* in leaves for timely flowering in *Brachypodium distachyon*

**Shu Liu** [1], **Siyi Chen** [1], **Yang Zhou** [1], **Yuxin Shen** [1], **Zhengrui Qin** [1] and **Liang Wu** [1,2,*]

1 State Key Laboratory of Rice Biology, College of Agriculture and Biotechnology, Zhejiang University, Hangzhou, Zhejiang 310058, China
2 Hainan Yazhou Bay Seed Laboratory, Hainan Institute, Zhejiang University, Sanya, Hainan 572000, China

*Author for correspondence: liangwu@zju.edu.cn
The author(s) responsible for distribution of materials integral to the findings presented in this article in accordance with the policy described in the Instructions for Authors (https://academic.oup.com/plcell/) is: L.W. (liangwu@zju.edu.cn)

## Abstract

FLOWERING PROMOTING FACTOR1 (FPF1), a small protein without any known domains, promotes flowering in several plants; however, its functional mechanism remains unknown. Here, we characterized 2 FPF1-like proteins, FPL1 and FPL7, which, in contrast, function as flowering repressors in *Brachypodium distachyon*. FPL1 and FPL7 interact with the components of the florigen activation complex (FAC) and inhibit FAC activity to restrict expression of its critical target, *VERNALIZATION1* (*VRN1*), in leaves, thereby preventing overaccumulation of FLOWERING LOCUS T1 (FT1) at the juvenile stage. Further, VRN1 can directly bind to the *FPL1* promoter and repress *FPL1* expression; hence, as VRN1 gradually accumulates during the late vegetative stage, FAC is released. This accurate feedback regulation of *FPL1* by VRN1 allows proper *FT1* expression in leaves and ensures sufficient FAC formation in shoot apical meristems to trigger timely flowering. Overall, we define a sophisticated modulatory loop for flowering initiation in a temperate grass, providing insights toward resolving the molecular basis underlying fine-tuning flowering time in plants.

## Introduction

Plants integrate multiple environmental and endogenous cues, such as day length, temperature, plant hormones, and nutrition, to initiate flowering. *FLOWERING LOCUS T* (*FT*), which encodes a phosphatidylethanolamine binding protein that acts as a florigen, has key functions in flowering time regulation. In the model plants, Arabidopsis (*Arabidopsis thaliana*) and rice (*Oryza sativa*), *FT* and its orthologs are produced in leaves and then transported through the phloem to the shoot apical meristem (SAM), where they interact with the bZIP transcription factor, FD, with the assistance of a 14-3-3 scaffold protein to form a florigen activation complex (FAC) in the nucleus. FAC then triggers the expression of a subset of floral meristem identity genes, such as *APETALA1* (*AP1*), to initiate floral onset (Abe *et al*. 2005; Wigge *et al*. 2005; Li and Dubcovsky 2008; Taoka *et al*. 2011; Li *et al*. 2015).

*Brachypodium distachyon*, an obligate long-day grass, serves as an ideal model for investigating flowering machinery in cereals due to its smaller size compared with wheat (*Triticum aestivum*) and barley (*Hordeum vulgare*). *FT1* is the closest ortholog of *FT* in *B. distachyon* and is induced under long-day conditions (LDs) to upregulate *VERNALIZATION1* (*VRN1*), a homolog of *AP1*, and other MADS box genes like *FRUITFULL2* (*FUL2*) to initiate the transition from vegetative to reproductive growth by assembling FAC in a manner that is relatively conserved in other plants (Ream *et al*. 2014; Qin *et al*. 2019). Nevertheless, some specific properties of *FT* expression have been revealed in *B. distachyon* and received considerable attention; for example, a Pooideae-specific microRNA, miR5200, that silences *FT1* and *FT2* to mediate photoperiodic control of flowering was discovered in *B. distachyon* (Wu *et al*. 2013).

Received February 16, 2023. Accepted June 26, 2023. Advance access publication June 28, 2023

## IN A NUTSHELL

**Background:** Timely flowering is critical for plant reproductive success. FLOWERING PROMOTING FACTOR1 (FPF1), a small protein without any known domains, has been shown to promote flowering in several plants, including Arabidopsis (*Arabidopsis thaliana*), tobacco (*Nicotiana tabacum*), and rice (*Oryza sativa*); however, the mechanism by which FPF1 functions remains unknown.

**Question:** How do FPF1 and FPF1-Like (FPL) proteins regulate flowering time in the model temperate grass *Brachypodium distachyon*?

**Findings:** We characterized 2 *B. distachyon* FPF1-like proteins, FPL1 and FPL7. In contrast to FPF, which promotes flowering in several plants, FPL1 and FPL7 repress flowering under long-day conditions in *B. distachyon*. FPL1 and FPL7 interact with the components of the florigen activation complex (FAC) and complex formation as well as its activity to restrict expression of its critical target, *VERNALIZATION 1* (*VRN1*), in leaves, thereby preventing subsequent overaccumulation of FLOWERING LOCUS T 1 (FT1) at the juvenile stage to avoid premature flowering. At the late vegetative stage, VRN1 directly binds the *FPL1* promoter and represses *FPL1* expression as it gradually accumulates, thus allowing proper *FT1* expression in leaves and ensuring sufficient FAC formation in shoot apical meristems to initiate timely flowering.

**Next steps:** It will be interesting to investigate additional upstream regulators and the potential transport of FPL1 and FPL7 in grasses. In addition, the function of FPL1 orthologs in other plants remains to be determined.

*FLOWERING PROMOTING FACTOR1* (*FPF1*) encodes a small protein (12.6 kD) with no known functional domains that plays a positive role in flowering initiation in many species (Kania *et al.* 1997; Melzer *et al.* 1999; Smykal *et al.* 2004; Greenup *et al.* 2010; Wang *et al.* 2014; Guo *et al.* 2020). In Arabidopsis, *FPF1* overexpression leads to clear early flowering, but has no effects when endogenous gibberellic acid (GA) biosynthesis is inhibited under short-day conditions (SDs), suggesting that *FPF1*-regulated flowering is likely dependent on the GA pathway (Kania *et al.* 1997). Recently, another homolog of FPF1, ACCELERATOR OF INTERNODE ELONGATION1, was identified as a mediator of internode elongation initiation in response to GA treatment in rice, further implicating FPF1 in GA signaling (Nagai *et al.* 2020). Nevertheless, how FPF1 functions in GA-mediated flowering in Arabidopsis remains obscure to date, since *FPF1* is only expressed under LDs where GA has very limited influence on reproductive onset (Kania *et al.* 1997). Further, in mutants of CONSTANS (CO), a critical factor responsible for photoperiodic activation of *FT1*, *FPF1*, can no longer be induced by LDs (Schmid *et al.* 2003). In addition, the late-flowering phenotype of the *co* mutant could be corrected by constitutive expression of *FPF1*, implying possible involvement of FPF1 in the genetic control of flowering by day length downstream of CO (Melzer *et al.* 1999). To date, although many positive effects of FPF1 on flowering have been described in diverse plants, the molecular mechanism of FPF1 and the direct regulatory factors involved in flowering pathways remain unknown.

In this study, we characterized 2 FPF1-like proteins, FPL1 and FPL7, in *B. distachyon*. We found that *FPL1* and *FPL7* are highly expressed in leaves and function as repressors, rather than accelerators, of flowering under LDs. Mechanistically, FPL1 and FPL7 suppress FAC formation and activity, to prevent premature flowering when plants are at the juvenile stage, while such restriction is released under feedback regulation by VRN1 when plants grow to the late vegetative stage, to ensure timely triggering of flowering. These results contribute to unraveling how, where, and when FPF1 proteins act to control flowering in plants.

## Results

### FPL1 and FPL7 repress flowering under LDs

To investigate the biological roles of FPF1 in *B. distachyon*, we first constructed a phylogenetic tree comprising 9 FPLs found in *B. distachyon* and named the homologs based on their evolutionary distances related to Arabidopsis FPF1 (Supplemental Fig. S1). Arabidopsis *FPF1* is reportedly expressed in response to an inductive photoperiod (Kania *et al.* 1997); therefore, we examined the expression profiles of all *FPF1* orthologs in *B. distachyon* under LDs and SDs. We observed that *FPL1* and *FPL7* exhibited significantly higher expression than the other 7 orthologs, and both exhibited much higher levels in LDs than in SDs (Fig. 1A), suggesting potential functions for FPL1 and FPL7 under LDs.

To further analyze the photoperiodic expression patterns of *FPL1* and *FPL7*, we examined their diurnal rhythms within a day and found that both *FPL1* and *FPL7* displayed higher expression levels at each time point under LDs than SDs (Fig. 1B). Moreover, levels of *FPL1* and *FPL7* were both significantly reduced in mutants of *phyC* (Woods *et al.* 2014), a critical light receptor, further indicating that *FPL1* and *FPL7* are strictly induced by LDs in *B. distachyon* (Fig. 1C). However, when we evaluated *FPL1* and *FPL7* expression under GA treatment, no clear differences were observed compared

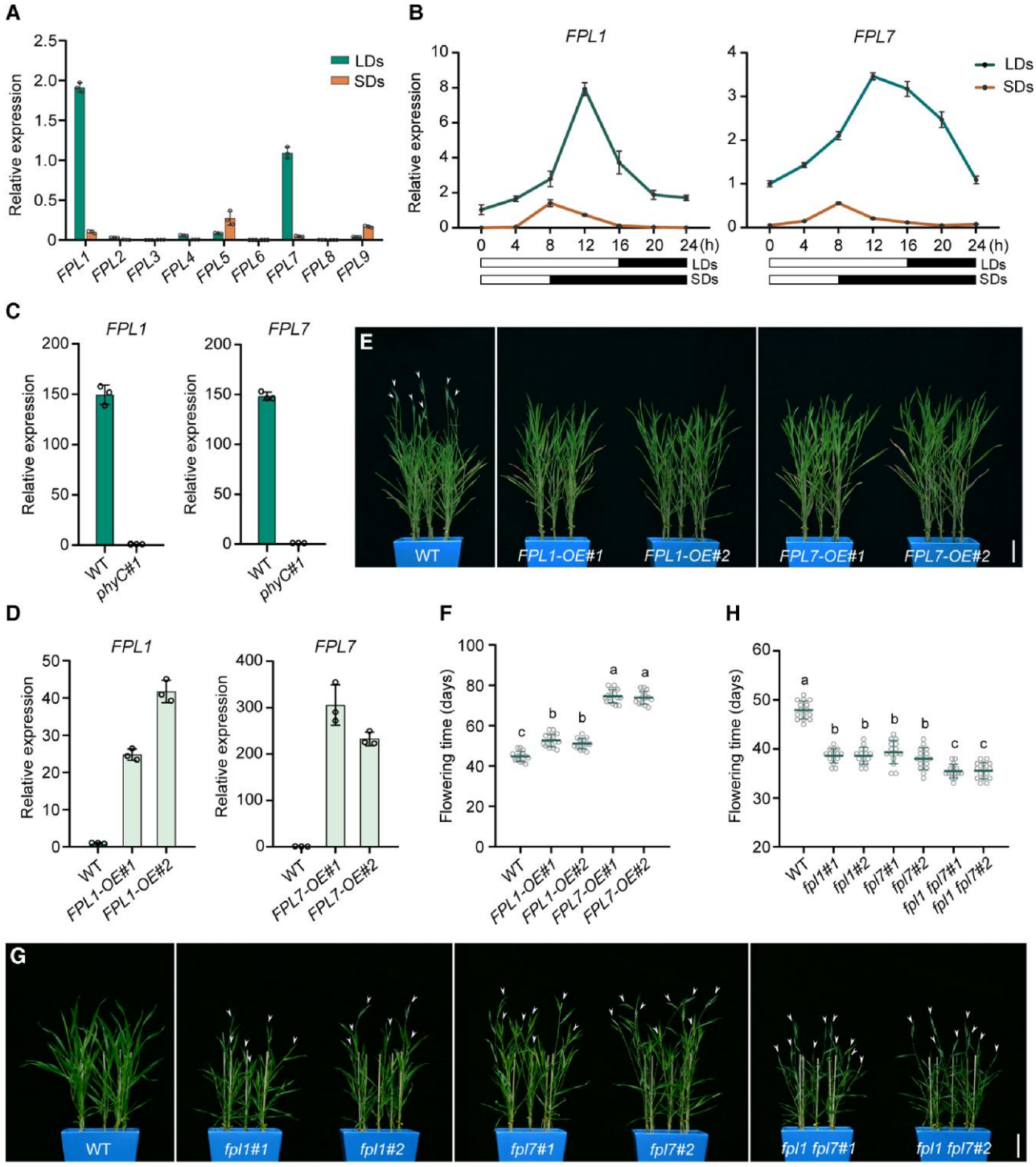


**Figure 1.** Long-day induced FPL1 and FPL7 inhibit flowering in *B. distachyon*. **A)** RT-qPCR analysis of the transcript levels of 9 *FPF1*-like genes in *B. distachyon* under LDs (22°C 16 h light/18°C 8 h dark) and SDs (22°C 8 h light/18°C 16 h dark). *UBC18* was used as an internal control for normalization of the RT-qPCR results. Error bars represent SD. **B)** Diurnal expression patterns of *FPL1* and *FPL7* under LDs and SDs. Abscissas represent the zeitgeber time (ZT) point. The white and black bars parallel to the horizontal axes represent light and dark periods, respectively. **C)** RT-qPCR analysis of *FPL1* and *FPL7* expression in WT Bd21-3 and *phyC-1* plants under LDs. **D)** RT-qPCR analysis of *FPL1* and *FPL7* expression in WT and the respective overexpression plants. **E)** Representative flowering phenotypes of WT, *FPL1-OE*, and *FPL7-OE* plants under LDs. White arrowheads point to spikes. Scale bars, 4 cm. **F)** Flowering time in WT, *FPL1-OE*, and *FPL7-OE* plants under LDs. Values marked with different letters indicate statistically significant differences (1-way ANOVA; $n = 15$ plants; $P < 0.0001$). **G)** Representative flowering phenotypes of WT, *fpl1*, *fpl7*, and *fpl1 fpl7* plants under LDs. White arrowheads point to spikes. Scale bars, 4 cm. **H)** Flowering time of WT, *fpl1*, *fpl7*, and *fpl1 fpl7* plants under LDs (1-way ANOVA; $n = 15$ plants; $P < 0.01$).

with mock-treated controls, regardless of day length, suggesting that *FPL1* and *FPL7* expression levels are insensitive to GA (Supplemental Fig. S2). Taken together, these results indicate that *B. distachyon* FPL1 and FPL7 are not controlled by GA, but are critically regulated by photoperiod.

To explore the biological functions of *B. distachyon* FPL1 and FPL7 in flowering control under LDs, we generated transgenic plants overexpressing the proteins under the control of a *Ubiquitin* promoter (Fig. 1D). We observed a clear delay of flowering in lines overexpressing *FPL1* and *FPL7* (*FPL1-OE* and *FPL7-OE*) relative to wild-type (WT) plants in LDs (Fig. 1, E and F), suggesting that FPL1 and FPL7 may inhibit flowering in *B. distachyon*. Next, we created *fpl1* and *fpl7* mutants using the CRISPR/Cas9 approach, to analyze the effects of *FPL1* and *FPL7* deficiency on flowering (Supplemental Fig. S3). Both *fpl1* and *fpl7* loss-of-function mutants flowered ~9 d earlier than WT plants, while *fpl1 fpl7* double mutants exhibited even more rapid flowering, at ~12 d earlier than WT plants under LDs (Fig. 1, G and H), indicating that FPL1 and FPL7 have redundant effects in repressing flowering under LDs. Moreover, compared with WT plants, we found that, when spikes emerged, numbers of parent culm leaves were significantly reduced in *fpl1 fpl7* mutants, while they were increased in *FPL1-OE* and *FPL7-OE* plants (Supplemental Fig. S4).

We also determined the flowering date and final leaf numbers when plants with both gain- and loss-of-function of FPL1 and FPL7 were grown under SDs and found that they were comparable with those of WT plants (Supplemental Fig. S5). Collectively, these results demonstrate that FPL1 and FPL7 function to inhibit the reproductive transition under LDs in *B. distachyon*.

## FPL1 and FPL7 interact with FAC components

To explore the molecular mechanism underlying the function of FPL1 and FPL7 as flowering repressors in *B. distachyon*, we cloned a number of genes with potential flowering control functions and performed a yeast 2-hybrid (Y2H) assay to search for FPL1 and FPL7 interactors. Intriguingly, we observed that the florigen protein, FT1, could physically interact with both FPL1 and FPL7 in yeast cells (Fig. 2A). Subsequent firefly luciferase (LUC) complementation imaging (FLCI), bimolecular fluorescence complementation (BiFC), and co-immunoprecipitation (Co-IP) assays further confirmed these interactions (Figs. 2, B to D, S6, and S7). Interestingly, analysis of the subcellular location of FPL1/7 and FT1 complexes indicated that they were primarily associated in the nucleus (Fig. 2C), although each protein separately was distributed evenly between the nucleus and cytoplasm (Supplemental Fig. S8), suggesting that there may be other factors involved in the interactions and mediating the subcellular location of the complex.

Since FT associates with FD and 14-3-3 proteins to assemble the canonical FAC in the nucleus (Deng *et al.* 2015; Li *et al.* 2015), we speculated that FD1 and 14-3-3 proteins may also be involved in the interactions between FT1 and FPL1/7. To test this hypothesis, we examined whether FPL1 and FPL7 could bind to FD1 or Gf14b, a critical 14-3-3 protein, using FLCI, BiFC, and Co-IP assays. We found that both FPL1 and FPL7 associated with FD1 and Gf14b and that the interactions between FPL1/7 and FD1 occurred mainly in the nucleus (Supplemental Figs. S9 and S10), suggesting that FPL1 and FPL7 interact with all components of FAC.

## FPL1 and FPL7 interfere with FAC formation and activity

As FPL1 and FPL7 function as flowering repressors and interact with FAC, we next asked whether they regulate flowering by influencing FAC formation or activity. To test the effects of FPL1 or FPL7 on FAC assembly, we performed LUC activity assays in *Nicotiana benthamiana* leaves to examine whether FPL1 or FPL7 could inhibit the interactions between pairs of FAC components. Compared with the introduction of a negative control (GFP), we detected significant decrease in interaction signals between FT1 and FD1, FT1 and GF14b, and FD1 and GF14b, when either FPL1 or FPL7 was transiently expressed in *N. benthamiana* leaves (Figs. 3, A and B, S11, and S12A). Subsequently, we used BiFC assays to further assess this effect and found a similar reduction of fluorescence signal, including its quantity and intensity, when FPL1 or FPL7 was introduced relative to the GUS control (Figs. 3, C and D, and S12B).

To further demonstrate the interruption of FAC formation by FPL1 and FPL7, we performed an in vitro competitive pull-down assay, to exclude the possibility that internal interfering factors, such as DNA and proteins in *N. benthamiana* leaves, affected the results of our previous experiments. Previous reports have suggested that FT could directly bind to 14-3-3 protein for translocation from the cytoplasm to the nucleus (Taoka *et al.* 2011), and we found that the interaction between *B. distachyon* FT1 and GF14b was remarkably inhibited when they were mixed with FPL1 and FPL7 proteins (Fig. 3E). Together, these results indicate that the formation of FAC can be blocked by FPL1 and FPL7.

Since FPL1 and FPL7 can interact with FD1, the transcription factor that directly binds to the promoter of FAC targets, we next investigated whether FPL1 and FPL7 could interfere with the association between FD1 and the *cis*-elements of VRN1. To test this hypothesis, we performed an electrophoretic mobility shift assay (EMSA) with fragments of the *VRN1* promoter containing a G-box (CACGTC) element associated with FD (Foster *et al.* 1994; Li and Dubcovsky 2008; Li *et al.* 2015; Collani *et al.* 2019; Romera-Branchat *et al.* 2020). Clear binding of FD1 to the *VRN1* promoter was observed, and the intensity of the mobility shift severely decreased when GST-FPL1 or GST-FPL7 was added to the mixture, compared with control GST (Figs. 4A and S13A), suggesting that FPL1 and FPL7 can disrupt binding of FD1 to its target *cis*-elements in the *VRN1* promoter.

Similarly, we further performed an EMSA including all 3 FAC components (His-FD1, His-FT1, and His-Gf14b) with the same *VRN1* fragment probe and found that GST-FPL1

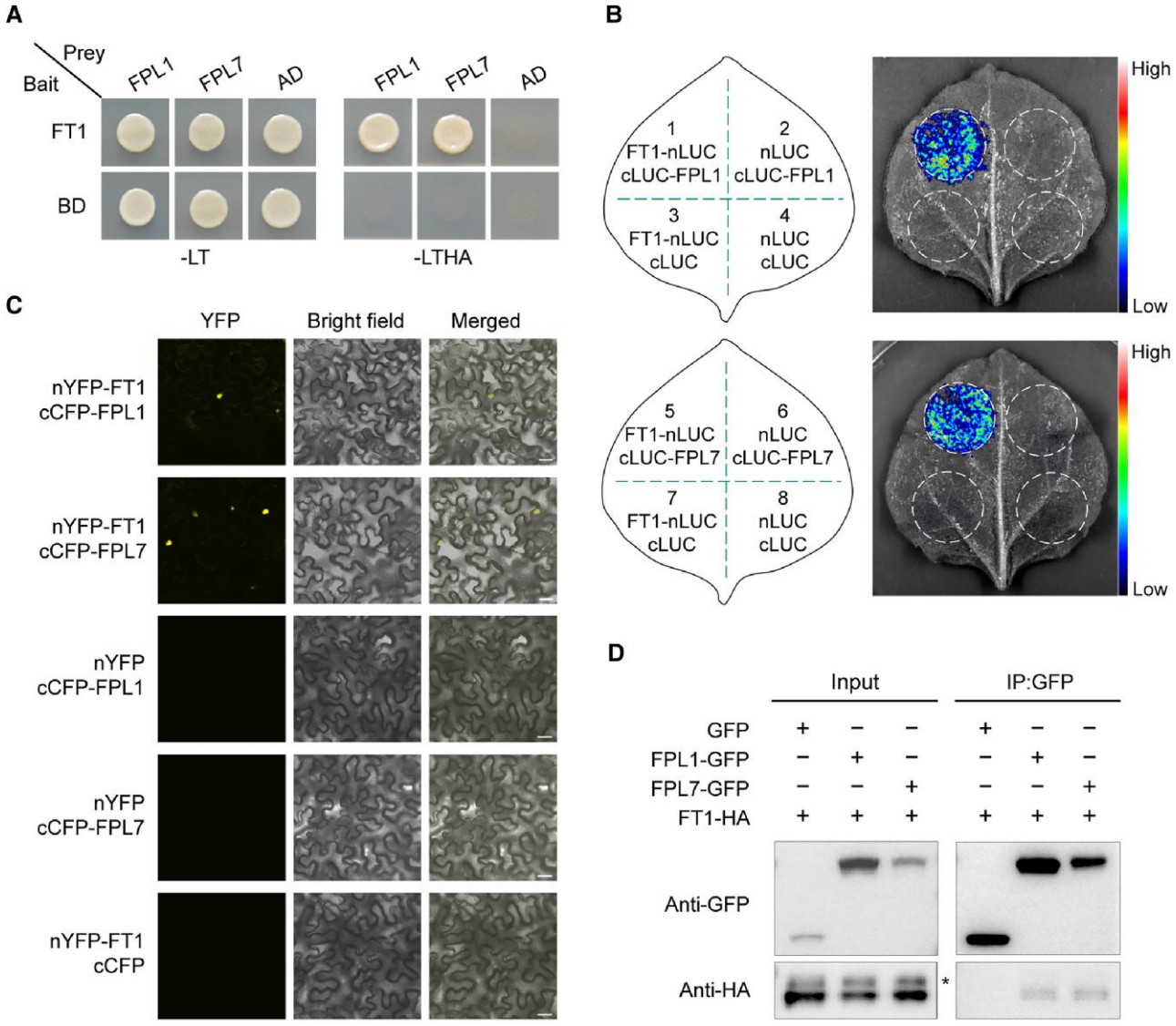


**Figure 2.** FPL1 and FPL7 interact with FT1. **A)** Analysis of FPL1/7 interaction with FT1 in yeast cells. Yeast cells growing on selective media without Leu, Trp, His, and Ade (-LTHA) represent positive interactions. **B)** FLCI assays of FPL1/7 and FT1 interactions in *N. benthamiana* leaves. **C)** BiFC assays of the interactions between FPL1/7 and FT1 in *N. benthamiana* leaf cells. Scale bar, 30 $\mu$m. **D)** In vivo Co-IP assays of the interactions between FPL1/7 and FT1. FPL1/7-GFP was coexpressed with FT1-HA in *N. benthamiana* leaves. GFP was used as a negative control, and the asterisk indicates non-specific bands.

or GST-FPL7 caused an analogous reduction in intensity of the mobility shift, while GST did not (Fig. 4B), indicating that the association of FAC with its target DNA element in *VRN1* promoter can be arrested by FPL1 and FPL7. It is noteworthy that the intensity decreases of *VRN1* probe bound by FAC were not accompanied by an enhancement of the shift beneath it, representing probe bound by FD1 that putatively deassociated from FAC (Figs. 4, C and D, and S13B). This may be attributable to FPL1 and FPL7 direct repression on the interaction between FD1 and its target *cis*-elements stated above.

The negative effect of FPL1 and FPL7 on FAC formation and target-binding process likely disrupts the transcriptional activation capacity of FAC; therefore, we performed LUC reporter assays to determine whether FPL1 or FPL7 can suppress the transactivation ability of FAC on the *VRN1* promoter. Compared with the negative control, we observed that firefly LUC intensity generated by FAC-mediated activation of *ProVRN1:LUC* was remarkably compromised when FPL1 or FPL7 were coinfiltrated (Figs. 4, E and F, and S14), suggesting an impairment of FAC transcriptional activation capacity caused by FPL1 or FPL7.

Together, our data indicate that interactions between FPL1 and FPL7 with FAC components are both detrimental to FAC assembly and interrupt FAC binding of DNA elements, thereby impairing the ability of FAC to activate

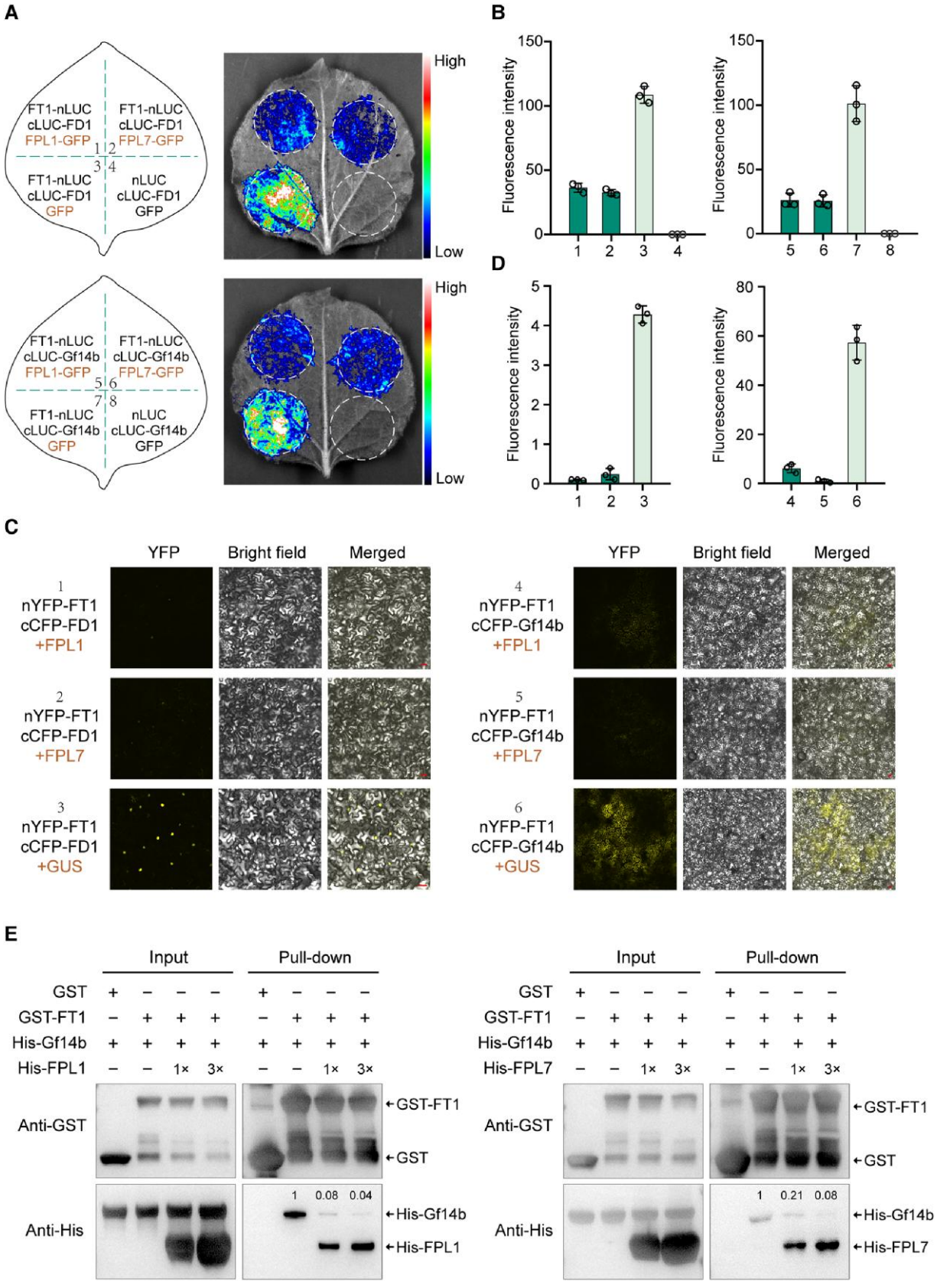


**Figure 3.** FPL1 and FPL7 inhibit FAC formation. **A)** LUC activity assays show that FPL1/7 represses the interactions of FT1 with FD1 (upper) and Gf14b (lower) in *N. benthamiana* leaves. GFP was used as a control. The white dotted circles indicate the region of interest (ROI) area for signal intensity quantification in **B)**. **B)** Relative LUC intensity analysis of experiments shown in **A)**. **C)** BiFC assays show that FPL1/7 attenuates the

(continued)

downstream genes, consequently leading to retardation of flowering.

## FPL1 and FPL7 downregulate *VRN1* and *FT1* expression in leaves

To investigate where *FPL1* and *FPL7* function, we analyzed their spatial expression profiles in leaves, SAM, and immature young panicles. We found that *FPL1* and *FPL7* mRNA were most abundant in leaves, whereas levels were negligible in the SAM and young panicles (Figs. 5A and S15A).

In Arabidopsis, *FD* and *AP1* are specifically expressed in the SAM (Wigge *et al.* 2005); however, in *B. distachyon*, we found that both *FD1* and *VRN1* were also expressed in leaves, in addition to the SAM, suggesting that FAC might also be formed and induce *VRN1* in leaves in this species (Figs. 5A and S15B). Moreover, we verified upregulation of *VRN1* transcription in leaves of *FT1* overexpression lines (Ream *et al.* 2014), whereas *VRN1* expression was decreased in leaves of plants overexpressing miR5200, which significantly reduces *FT1* mRNA levels (Supplemental Fig. S16, A and B) (Wu *et al.* 2013). These results imply that FPL1 and FPL7 may suppress *VRN1* expression by disrupting FAC function in leaves. To test this hypothesis, we examined *VRN1* expression levels in *FPL1* and *FPL7* gain-of-function and loss-of-function plants. As expected, *VRN1* levels were significantly decreased in leaves overexpressing *FPL1* and *FPL7*, while they were increased in *fpl1* and *fpl7* single and double mutants (Fig. 5, B and C), indicating that FPL1 and FPL7 impair FAC transcriptional activation of *VRN1* in *B. distachyon* leaves.

Previous studies have implied that VRN1 can accumulate in leaves, leading to feedback upregulation of *FT1* in barley and wheat (Hemming *et al.* 2008; Chen and Dubcovsky 2012; Ream *et al.* 2014; Deng *et al.* 2015; Woods *et al.* 2016). We confirmed these results in *B. distachyon*, as we found that *FT1* is significantly induced in leaves overexpressing *VRN1* (*VRN1-OE*) (Ream *et al.* 2014), while levels were severely reduced in leaves of *vrn1* mutants generated using a CRISPR/Cas9 approach (Supplemental Fig. S16, C to G). Based on these findings, we speculate that the reduced *VRN1* levels caused by *FPL1* and *FPL7* repression may ultimately lead to decreased FT1 abundance in leaves. Indeed, we observed that *FT1* expression levels were significantly reduced in leaves of plants overexpressing *FPL1* or *FPL7*, whereas levels were dramatically increased in *fpl1* and *fpl7* single and double mutants (Fig. 5, D and E), suggesting possible roles for FPL1 and FPL7 in downregulation of *FT1* via inhibition of *VRN1* in *B. distachyon* leaves. In addition, we detected altered *VRN1* expression levels in SAMs, consistent with those of *FT1* in leaves, from gain- and loss-of-function of *FPL1* and *FPL7* plants (Supplemental Fig. S17), because the FT1 protein was transported from leaves to SAMs, where it formed a novel FAC complex to induce *VRN1*.

To further genetically validate the roles of *FPL1* and *FPL7* in repressing *FT1* expression, we generated triple mutants of *ft1 fpl1 fpl7* and observed their flowering performance under LDs (Supplemental Fig. S18). The early flowering phenotype of *fpl1 fpl7* was completely abolished when a deletion of *FT1* was introduced, and the triple mutants displayed a severe delay in flowering and could hardly bear seeds, similar to the phenotype of *ft1* mutant (Figs. 5, F and G, and S19). In addition, we performed a transcriptomic analysis of *fpl1 fpl7*, *FT1-OE*, and *VRN1-OE* leaves, to screen for overlapping regulatory genes. Strikingly, among 380 overlapping differentially expressed genes, *FUL2* and *FUL3* were remarkably upregulated, while *MADS56* was repressed (Fig. 5H and Supplemental Data Set 1), suggesting that loss-of-function of FPL1 and FPL7 and gain-of-function of FT1 and VRN1 can lead to a similar regulation of downstream flowering genes in *B. distachyon* leaves.

Overall, these data demonstrate FPL1 and FPL7 repress *VRN1* via inactivation of FAC, thereby meditating subsequent feedback control of *FT1* expression in leaves for flowering initiation.

## VRN1 represses *FPL1* at the late vegetative stage

To clarify when FPL1 and FPL7 interfere with FAC, we examined their temporal expression patterns every 2 wks. While *FPL1* and *FPL7* expression levels apparently decreased in leaf tissues, those of *VRN1* and *FT1* gradually increased during the entire vegetative stage (Figs. 6A and S20). This observation explains how FPL1 and FPL7 mediate flowering control in *B. distachyon* by negatively regulating flowering through inhibition of *FT1* and *VRN1* at the juvenile stage, whereas they may lose this ability later, ensuring sufficient *FT1* expression before flowering transition.

In light of this finding, we considered it critical to identify upstream factors that downregulate *FPL1* and *FPL7* expression after the juvenile stage. According to the opposite temporal expression patterns of *VRN1* and *FPL1/7* in leaves, we speculate whether VRN1 could directly repress *FPL1* and *FPL7* through feedback regulation as a transcription factor. To test this hypothesis, we performed EMSA to detect the association of VRN1 with the *FPL1* and *FPL7* promoters around CArG box motif, the typical binding site for MADS box transcription factors (Riechmann *et al.* 1996; Riechmann and Meyerowitz 1997; Deng *et al.* 2015). An obvious mobility shift was observed when a fragment of the *FPL1* promoter containing a CArG motif was mixed with purified MBP-VRN1

**Figure 3.** (Continued)
interactions of FT1 with FD1 (left) and Gf14b (right) in *N. benthamiana* leaves. GUS was used as a control. Scale bar, 30 $\mu$m. **D)** Relative fluorescence intensity analysis of experiments shown in **C)**. **E)** Competitive GST pull-down assays show that FPL1/7 inhibits direct interactions between FT1 and Gf14b. His-FPL1 and His-FPL7 (1- and 3-fold) were mixed with GST-FT1 and His-Gf14b for competition. GST was used as a negative control, and the numbers above the lanes indicate relative band intensity quantified by ImageJ.

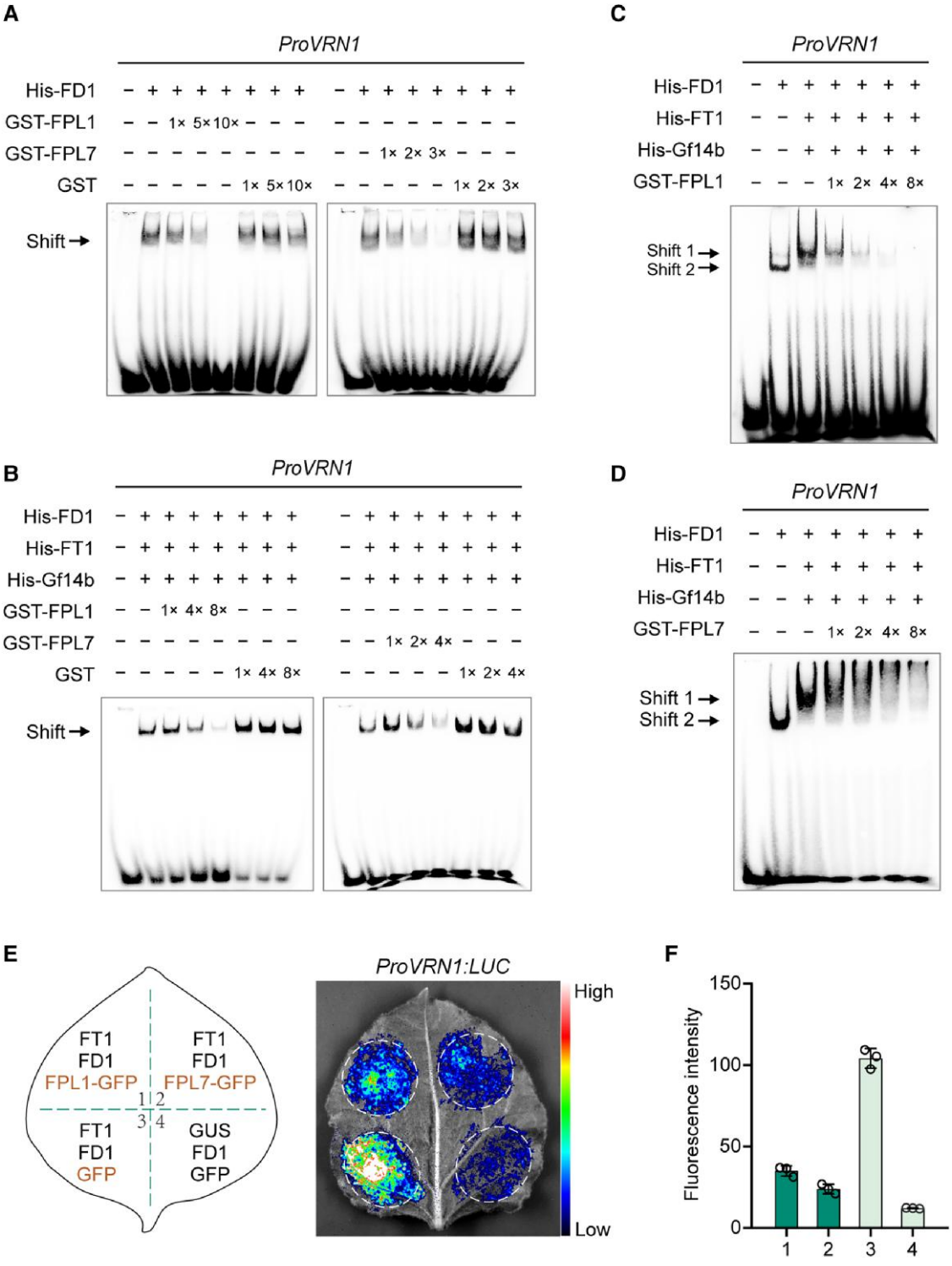


**Figure 4.** FPL1 and FPL7 impair FAC activation of the *VRN1* promoter. **A)** EMSAs indicate that FPL1/7 attenuates binding of FD1 to *cis*-element of *VRN1* promoter. The arrow indicates the protein–DNA complex. GST-FPL1 (1-, 5-, and 10-fold) or GST-FPL7 (1-, 2-, and 3-fold) was mixed with His-FD1 for competition. GST was used as a control. **B)** EMSA indicates that FPL1/7 attenuates binding of FAC to *cis*-element of *VRN1* promoter. The arrow indicates the protein–DNA complex. GST-FPL1 (1-, 4-, and 8-fold) or GST-FPL7 (1-, 2-, and 4-fold) were mixed with His-FD1, His-FT1, and His-Gf14b for competition. GST was used as a control. **C)** and **D)** EMSA indicates that FPL1 **C)** and FPL7 **D)** repress the associations of both FD1 and FAC complex with *cis*-element of *VRN1* promoter. Shift 1 and Shift 2 indicate *VRN1* probes bound by FAC and FD1, respectively. GST-FPL1 and GST-FPL7 (1-, 2-, 4-, and 8-fold) were mixed with FAC components for competition. **E)** Transactivation assays show that FPL1/7 impairs transactivation ability of FAC on the *VRN1* promoter. GFP and GUS were used as controls. The white dotted circles indicate the ROI for signal intensity quantification in **F)**. **F)** Relative LUC intensity analysis of experiment shown in **E)**.

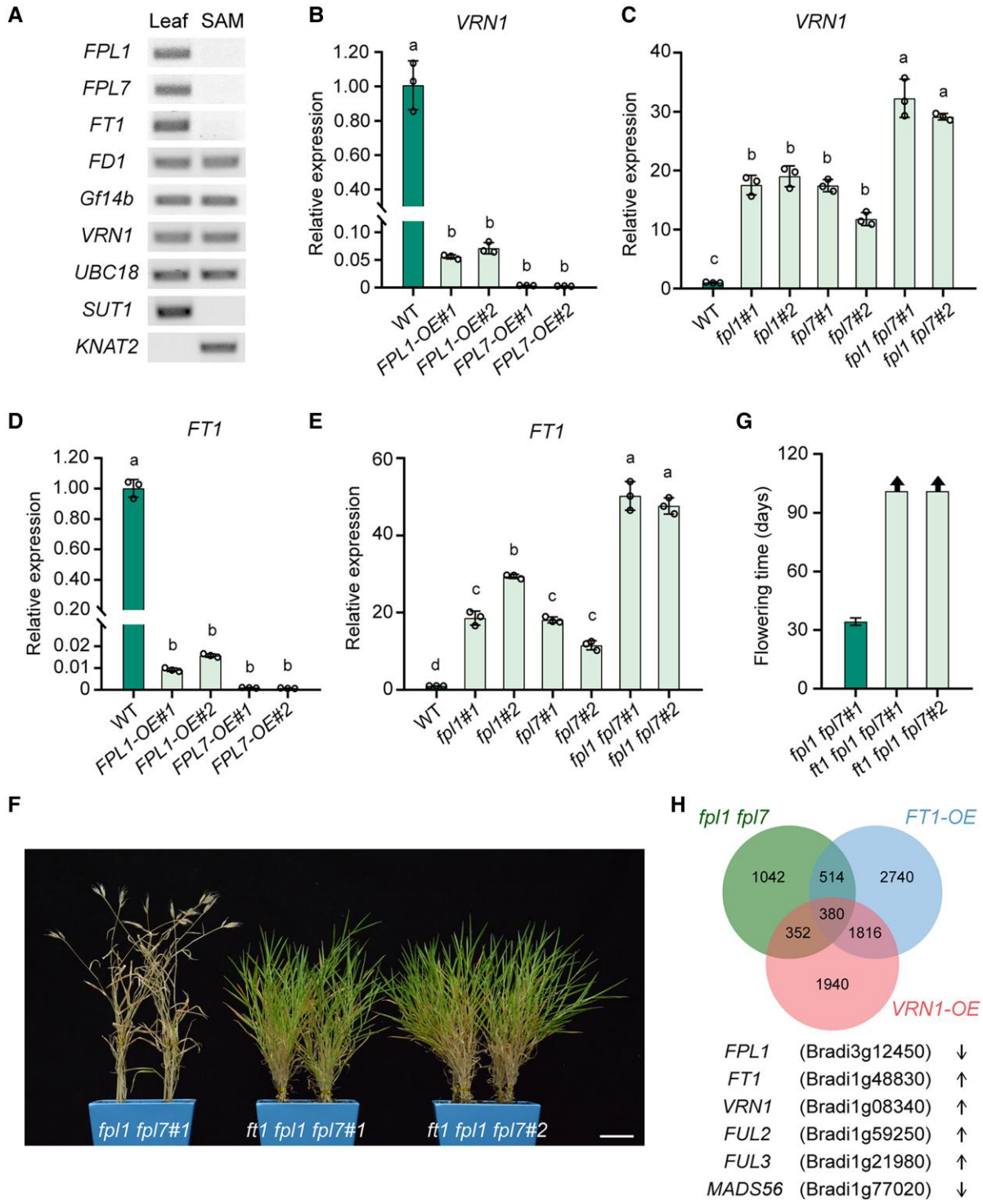


**Figure 5.** FPL1 and FPL7 downregulate *FT1* and *VRN1* expression in leaves. **A)** RT-PCR analysis of the spatial expression levels of *FPL1/7*, *FT1*, *FD1*, *Gf14b*, and *VRN1* in leaf and SAM. *UBC18*, leaf-specific *SUT1*, and SAM-specific *KNAT2* were used as controls to verify sample quality and specificity. **B)** RT-qPCR analysis of *VRN1* expression in leaves of WT and *FPL1/7* overexpression lines under LDs (1-way ANOVA; $P < 0.0001$). **C)** RT-qPCR analysis of *VRN1* expression in leaves of WT and single and double mutants of *fpl1* and *fpl7* under LDs (1-way ANOVA; $P < 0.0001$). **D)** RT-qPCR analysis of *FT1* expression in leaves of WT and *FPL1/7* overexpression lines under LDs (1-way ANOVA; $P < 0.0001$). **E)** RT-qPCR analysis of *FT1* expression in leaves of WT and single and double mutants of *fpl1* and *fpl7* under LDs (1-way ANOVA; $P < 0.001$). **F)** Representative flowering phenotypes of *fpl1 fpl7* and *ft1 fpl1 fpl7* mutants under LDs. *ft1 fpl1 fpl7* mutants showed a severe delay in flowering compared with *fpl1 fpl7*. Scale bars, 4 cm. **G)** Flowering time of *fpl1 fpl7* and *ft1 fpl1 fpl7* mutants under LDs. *ft1 fpl1 fpl7* could not flower over 3 months ($n = 15$ plants). **H)** Overview of genes differentially expressed in *fpl1 fpl7*, *FT1-OE*, and *VRN1-OE*, with 380 overlapping genes among 3 RNA-Seq data sets. Several common differentially expressed genes were highlighted below.

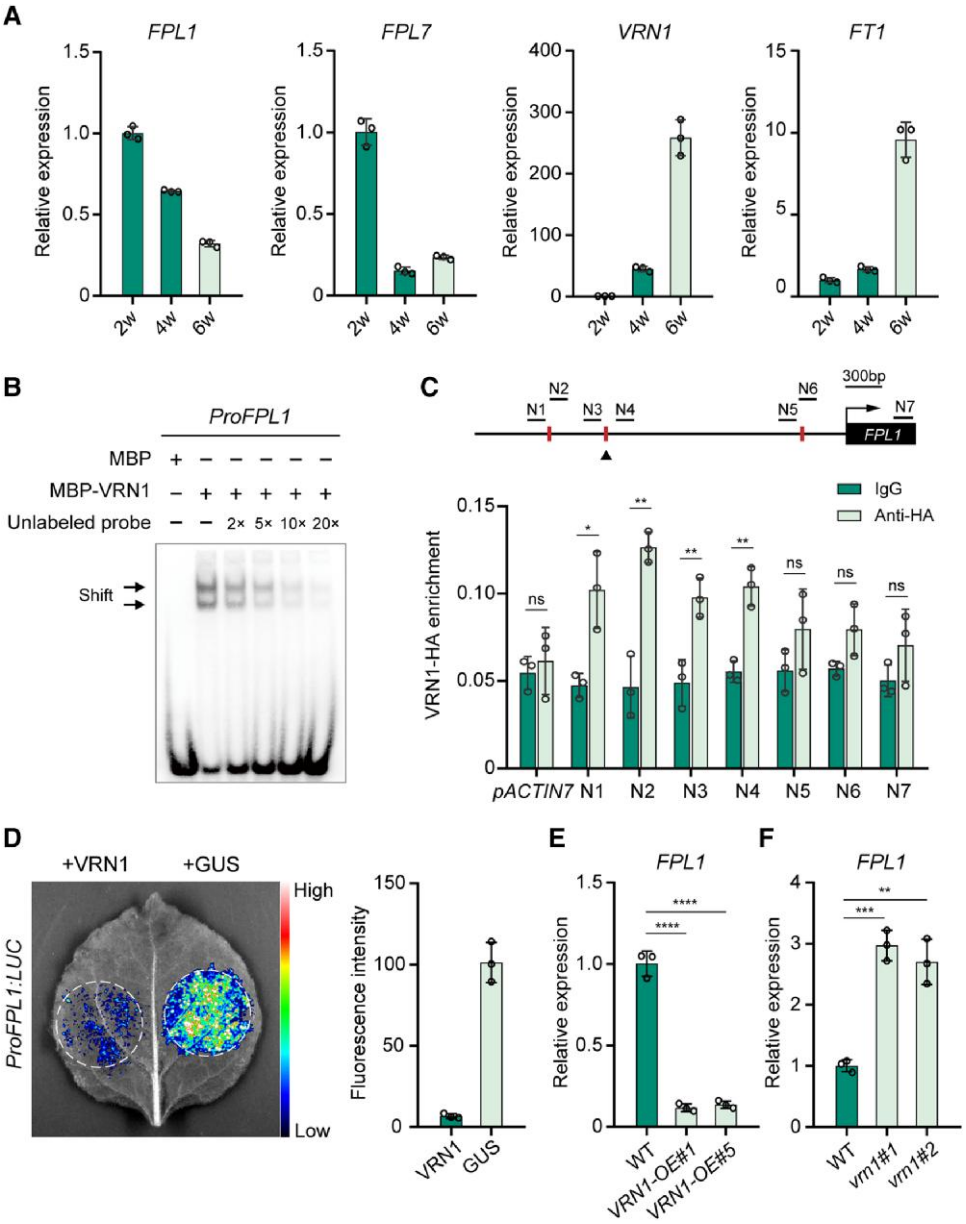


**Figure 6.** VRN1 directly represses *FPL1* at the late vegetative stage. **A)** RT-qPCR analysis of *FPL1*, *FPL7*, *VRN1*, and *FT1* expression levels in 2-, 4-, and 6-wk-old Bd21 leaves. **B)** EMSA indicates the direct interaction between VRN1 (monomer and dimer) and the *FPL1* promoter. The arrow indicates the mobility shift. Unlabeled 2-, 5-, 10-, and 20-fold excess probes were used for competition. MBP was used as a control. The position of segment to design probe in *FPL1* promoter is shown in **C)**. **C)** ChIP-qPCR analysis of VRN1 enrichment on the *FPL1* promoter. The assay was performed using leaves from *VRN1-HA* transgenic plants. Scale diagram of the *FPL1* promoter (3 kb) is shown above with 3 CArG motifs marked by red bars and fragments used for qPCR marked by black bars. The triangle indicates the position of the EMSA probe used in **B)**. ChIP values were normalized to corresponding input DNA. The *Actin7* promoter was used as a negative control (Student's *t* test; $^{*}P < 0.05$; $^{**}P < 0.01$; ns, not significant). **D)** Transactivation assays show that VRN1 represses *FPL1* transcription in *N. benthamiana* leaves. GUS was used as a control. The white dotted circles indicate the ROI area for signal quantification. **E)** RT-qPCR analysis of *FPL1* expression in WT Bd21-3 and *VRN1* overexpression lines under LDs. Leaf samples were harvested from plants grown for 3 wks (Student's *t* test; $^{****}P < 0.0001$). **F)** RT-qPCR analysis of *FPL1* expression in WT and *vrn1* mutants under LDs (Student's *t* test; $^{**}P < 0.01$, $^{***}P < 0.001$).

and excess unlabeled probe could compete and readily eliminate the shifted band (Fig. 6B). Next, we generated *VRN1-HA* transgenic plants and immuno-purified VRN1-associated DNA using an anti-HA antibody, which provided further evidence supporting the interaction between VRN1 and *FPL1* promoter fragments, but not with a negative control (Figs. 6C and S21A).

Subsequently, we determined the effect of VRN1 on *FPL1* transcription. A LUC reporter assay in *N. benthamiana* leaves demonstrated that VRN1 dramatically attenuated transcriptional

activity of the *FPL1* promoter compared with negative control (Fig. 6D). Further, we observed significantly reduced *FPL1* expression in lines overexpressing *VRN1*, while *FPL1* levels were profoundly enhanced in *vrn1* mutants (Fig. 6, E and F). Nevertheless, we did not detect notable promotion of *FPL7* expression in *vrn1* mutants (Supplemental Fig. S21B), although there was a weak association of VRN1 with the first CArG motif in the *FPL7* promoter in EMSA and chromatin immunoprecipitation (ChIP)-PCR assays (Supplemental Fig. S21, C to D), indicating that factors other than VRN1 may regulate the temporal expression of *FPL7*. Together, these results suggest that VRN1 can directly inhibit *FPL1* expression via a feedback regulation mechanism, which may facilitate its release from inhibition by FPL1 at the late stage of vegetative growth, to initiate flowering.

## Discussion

FPF1 has long been considered a positive regulator of flowering; however, its function in the flowering pathway remains unknown (Kania *et al*. 1997; Melzer *et al*. 1999; Smykal *et al*. 2004; Greenup *et al*. 2010; Wang *et al*. 2014; Guo *et al*. 2020). Here, we present a regulatory module involving 2 members of the FPF1 protein family in *B. distachyon*, which behave as flowering repressors. FPL1 and FPL7 are highly expressed at the juvenile stage and prevent FAC assembly as well as repress the capacity of FAC to activate *VRN1*, thereby avoiding premature flowering, which is harmful to plants. When plants accumulate VRN1 at the late vegetative stage, FPL1 is diminished, as VRN1 can directly associate with *FPL1* promoter to inhibit its transcription, leading to enhanced FAC activity and elevated *VRN1* expression. The resulting increase of VRN1 abundance then promotes *FT1* expression in leaves, which ensures sufficient FT1 protein is transported to the SAM, where it constitutes another FAC, to activate inflorescence meristem identity genes and initiate reproductive transition (Fig. 7).

Interestingly, our data show that VRN1 cannot regulate FPL7 expression in the same way that it controls FPL1, although it interacted weakly with *cis*-elements in the *FPL7* promoter. As FUL2 in temperate grasses is also classified as a homolog of AP1 in Arabidopsis, FUL2, rather than VRN1, may act as an upstream regulator of *FPL7*, because FUL2 shows a stronger binding to CArG box in the *FPL7* promoter and represses its transcriptional activity (Supplemental Fig. S22). Further expression analysis of *FPL1* and *FPL7* in *ful2* and *vrn1ful2* mutants is required to clarify how VRN1 and FUL2 individually or collaboratively modulate *FPL1* and *FPL7* expression in *B. distachyon*. Furthermore, *FT1* levels increase throughout plant development, similar to *VRN1* and opposite to the temporal expression patterns of *FPL1* and *FPL7*; hence, whether the FT1 and FD1 module can inhibit FPL1 and FPL7 accumulation via a feedback loop warrants investigation.

The evolution of FPF1 orthologs appears to be extremely divergent among different plants. Firstly, FPF1 exhibits different flowering control functions; in Arabidopsis, rice, and many other plants, it accelerates flowering, while *B. distachyon* FPL1 represses flowering. Secondly, FPF1 exhibits different expression patterns; Arabidopsis *FPF1* is significantly enriched in the peripheral zone of undifferentiated organs, such as apical meristems, floral meristems, and axillary meristems (Kania *et al*. 1997). In contrast, *FPL1* in *B. distachyon* is expressed mainly in leaves. Thirdly, GA treatment can induce *ACE1*, the *FPF1* ortholog in rice (Nagai *et al*. 2020), whereas *FPL1* expression in *B. distachyon* is not influenced by GA treatment. We propose that these different gene expression patterns and protein structures may contribute to divergent functions of FPF1 family proteins in different plants. It will be helpful to define how such small plant-specific proteins evolve through further characterization FPF1 orthologs in other plants, in addition to those in *B. distachyon*.

Unlike in Arabidopsis, where FAC forms specifically in the SAM, in cereals, regulation of floral genes by FAC occurs in both the SAM and leaves, since *VRN1* is expressed at comparable levels in these 2 tissues (Alonso-Peral *et al*. 2011). A previous study proposed that *VRN1* may have dual roles in flowering initiation in temperate grasses. When expressed in the SAM, *VRN1* functions as a canonical florescence meristem identity gene, similar to *AP1*; however, when expressed in leaves, *VRN1* likely functions as an *FT1* regulator that induces *FT1* expression to initiate flowering (Hemming *et al*. 2008; Chen and Dubcovsky 2012; Ream *et al*. 2014; Deng *et al*. 2015; Woods *et al*. 2016). In this study, we propose that FAC may be formed in 2 tissues in *B. distachyon*, since *FD1* and *Gf14b* are expressed in both leaves and the SAM (Figs. 5A and S15B). Therefore, if FAC forms in leaves, it predominantly controls *FT1* expression via feedback regulation of *VRN1*, while FAC in meristem functions canonically to induce floral identity genes and establish flower development. Hence, FT1 and VRN1 may form a positive regulatory loop in cereal leaves, which may help them rapidly and substantially amplify their own protein levels, ultimately generating sufficient FT1 for transport to the SAM and initiating floral transition in a short period. Nevertheless, if this loop is released too early, the grasses may be unable to accumulate sufficient energy and nutrition for reproduction, which would be deleterious to their offspring. Accordingly, it is obligatory to restrict FT1 and VRN1 overaccumulation at the juvenile stage, and FPL1 and FPL7 have very important functions in this context as, when highly expressed, they can disable FAC, thus ensuring plants initiate reproductive growth at the appropriate time.

To date, only a few factors that interact with florigen have been identified, including those that assist in FT functions, such as FD, 14-3-3 proteins, SWEETs, and TCPs (Abe *et al*. 2005; Taoka *et al*. 2011; Ho and Weigel 2014; Abelenda *et al*. 2019; Nicolas *et al*. 2022), as well as those that facilitate transport of FT over short or long distances (Liu et al. 2012, 2019; Zhu et al. 2016). Given that FPL1 and FPL7 are also micro proteins (even smaller than FT), future investigations to determine whether they can be transported in an FT- or FT partner-dependent manner are warranted.

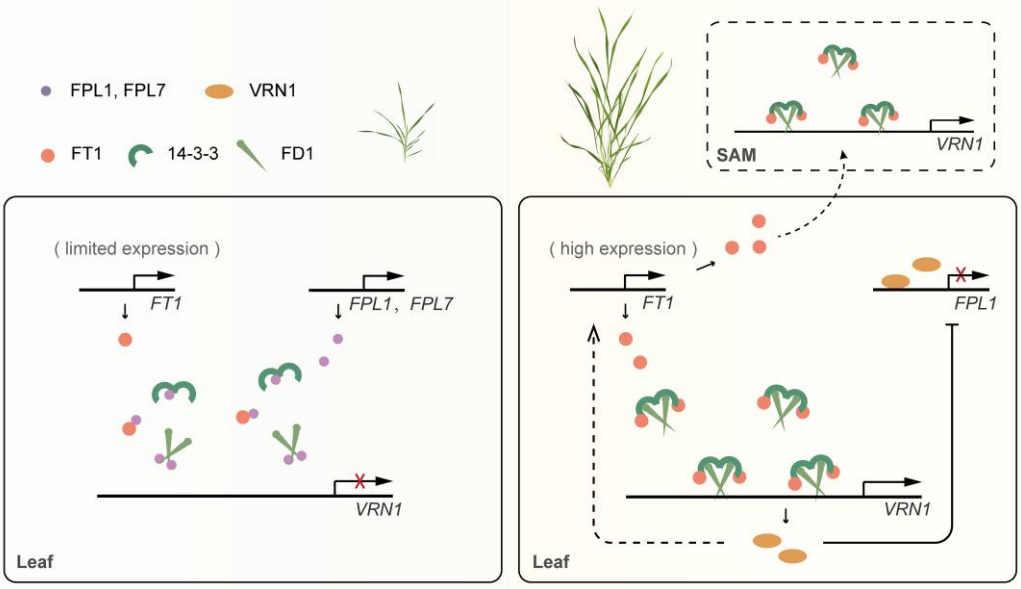


**Figure 7.** A proposed working model for the roles of FPL1 and FPL7 in *B. distachyon* flowering regulation. At the early juvenile stage, when their genes are highly expressed, abundant FPL1 and FPL7 proteins are generated and interact with FAC components, thereby preventing FAC assembly and repressing the capacity of FAC to activate *VRN1*. This leads to low *VRN1* expression in plant leaves, avoiding premature flowering. VRN1 protein can directly bind to the *FPL1* promoter; thus, as it gradually accumulates during plant development, it inhibits *FPL1* expression, thereby releasing FAC activity. Subsequently, the enhanced FAC activity in leaves triggers rapid induction of *VRN1* expression, which further promotes *FT1* transcription in plant leaves, resulting in sufficient FT1 proteins for transport to the SAM, where they activate floral pattern genes and initiate flowering when plants grow to the late vegetative stage.

## Materials and methods

### Plant materials and growth conditions

*B. distachyon* variety Bd21 was used in this study, unless otherwise noted. Plants were grown in growth chambers under long-day (22°C 16 h light/18°C 8 h dark) or short-day (22°C 8 h light/18°C 16 h dark) conditions with supplemental lighting (3,200 K fluorescent bulbs, 10,000 Lux). Flowering time was measured as the days when the seeds were sown to the date that the first spike visibly emerged from the sheath and final leaf number on the parent culm.

### Vector construction and plant transformation

Full-length coding sequences (CDS) of *FPL1* and *FPL7* were amplified from Bd21 cDNA and cloned into the binary vector, pCUBI1390, under the control of the maize (*Zea mays*) *UBIQUITIN* (*UBI*) promoter, to generate plants overexpressing the genes. Full-length *VRN1* CDS was cloned into the construct, *UBI:VRN1-HA*, to generate transgenic plants for the expression of VRN1 fused with a 3×HA tag for ChIP analysis. *FPL1*, *FPL7*, *FT1*, or *VRN1* target sequences in sgRNA expression cassettes were cloned into CRISPR/Cas9 system constructs to generate single, double, or triple mutants. Recombinant plasmids were transformed in Bd21 plants using *Agrobacterium tumefaciens* strain AGL1 and embryogenic callus derived from immature embryos. *B. distachyon* transformation was conducted as previously described (Alves *et al.* 2009). Sequencing analysis was performed to exclude off-target effects of the other *FPLs* in mutant plants of *FPL1* and *FPL7*. All primers used to construct genetic materials are listed in Supplemental Data Set 2.

### RNA expression analysis

At least 3 newly full-expanded leaves of plants grown in LDs for around 4 wks were harvested for gene expression analysis, unless otherwise noted. Leaf samples were pooled to extract RNA using RNAiso Plus (Takara). Total RNA was then reverse transcribed using reverse transcriptase with oligo (dT) primers (Promega). qPCR analysis was performed on a StepOnePlus real-time PCR system (ABI) with Power Up SYBR Master Mix (ABI), following the manual. *UBC18* was used as an internal control for normalization of RT-qPCR results. Three biological replicates and 3 technical repeats were conducted for every RT-qPCR assay. Primers used for gene expression analysis are listed in Supplemental Data Set 2.

For transcriptome analysis, 3 biological replicates of extracted RNA from leaves of *fpl1 fpl7*, *FT1-OE*, *VRN1-OE*, and their respective WT plants were used to perform RNA-sequencing on an Illumina HiSeq 4000 platform (LC-Bio Technology Co., Ltd., Hangzhou, China). Low-quality and vector sequences were removed using Trimmomatic (v0.35), and remaining clean data were aligned to the *B. distachyon* genome (Phytome genome ID:314) using HISAT2 (v2.1.0) with default parameters. DEseq (v1.20.0) was used for analysis of significantly differentially expressed genes, and $P < 0.05$ and $|\log_2 (\text{fold change})| > 0.5$

was set as the threshold for differential expression. The raw sequence data have been deposited in the Genome Sequence Archive in National Genomics Data Center (accession numbers: CRA010993, CRA011008, and CRA011009). Details of RNA-seq data are presented in Supplemental Data Set 1.

## Phylogenetic analysis

Protein sequences used for phylogenetic analysis were retrieved from public databases. Accession numbers are shown in Supplemental Fig. S1. Sequence alignments were produced using ClustalW, and phylogenetic trees were constructed using the MEGA program with the neighbor-joining method. Bootstrap values were measured based on 1,000 replications for each branch. Sequence alignment and tree files are provided as Supplemental File 1 and S2.

## Y2H assays

The *FT1* full-length CDS was amplified and cloned in pGBKT7. *FPL1* and *FPL7* full-length CDS were amplified and cloned in pGADT7. The recombinant plasmids were cotransformed into yeast strain, AH109, using a lithium acetate–based transformation protocol. Positive colonies grown on SD/-Leu/-Trp (-LT) medium were transferred onto selective SD/-Leu/-Trp/-His/-Ade (-LTHA) medium. Positive interactions on -LTHA medium were observed after incubation at 30°C for ~4 d.

## LUC imaging assays

To detect interactions between FPL1/7 and FAC components, full-length CDS of corresponding genes were amplified and ligated with *N*-terminal or *C*-terminal fragment of LUC. Constructed binary vectors were coexpressed in *N. benthamiana* leaves using *A. tumefaciens* strain EHA105, as described previously (Qin *et al.* 2017, 2019). Strains were resuspended to $OD_{600} = 0.6$ in infiltration buffer containing 150 $\mu$M acetosyringone, 10 mM $MgCl_2$, and 10 mM MES. To determine the effects of FPL1 and FPL7 on FAC formation, full-length *FPL1* and *FPL7* CDS were amplified and cloned into pCambia2300 and then coexpressed with the indicated FAC components to detect their influence on LUC intensity. LUC images were taken after 2 to 3 d using an imaging device (Tonon 5200).

For transactivation assays, 2 to 3 kb *VRN1*, *FPL1*, and *FPL7* promoter sequences were amplified and inserted into the pGreenII-0800-LUC vector. Full-length *FT1*, *FD1*, or *VRN1* CDS were amplified, cloned in pCAMBIA2300, and coexpressed in *N. benthamiana* leaves with corresponding promoter-LUC vectors to assess their transcriptional regulation ability. To detect the effects of FPL1 and FPL7 on FAC-triggered *VRN1* induction, *A. tumefaciens* strain EHA105 harboring FPL1 and FPL7 was expressed in the indicated groups and their influence on LUC intensity was detected. LUC images were taken after 2 to 3 d using an imaging device (Tonon 5200).

To ensure comparable expression of constructs in the aforementioned experiments, we adjusted all parallel *Agrobacterium* strains to the same OD and mixed them with equal-volume before injection. The corresponding RT-PCR assays were performed to measure each introduced gene expression level, with *Actin* used as an internal control for normalization.

## Subcellular location and BiFC assays

To detect protein subcellular location, full-length *FT1*, *FD1*, *Gf14b*, *FPL1*, or *FPL7* CDS were amplified, fused in-frame with GFP, and transiently expressed in *N. benthamiana* leaves through *Agrobacterium*-mediated transformation. Strains were resuspended to $OD_{600} = 0.6$ in infiltration buffer (described above). GFP-fused proteins were localized after 2 to 3 d using a confocal laser scanning microscope (Olympus FV3000).

For BiFC assays, full-length CDS of FAC components, as well as *FPL1* and *FPL7*, were amplified and cloned into vectors containing either nYFP or cCFP fragments and transiently coexpressed in *N. benthamiana* leaves through *Agrobacterium*-mediated transformation. Fluorescence signals were observed after 2 to 3 d using a confocal laser scanning microscope (Olympus FV3000).

## Co-IP assays

Total proteins from *N. benthamiana* leaves infected with the indicated constructs using *Agrobacterium* were isolated using extraction buffer containing 50 mM Tris-HCl (pH 7.5), 150 mM NaCl, 1 mM EDTA, 10% (*v*/*v*) glycerol, 0.1% NP-40, 1 mM phenylmethylsulfonyl fluoride, and 1× protease inhibitor cocktail (Roche). Supernatants were incubated with anti-GFP beads (Medical & Biological Laboratories) at 4°C for 2 h with gentle shaking. Beads were then washed 4 times with extraction buffer and boiled with SDS loading buffer for subsequent immunoblotting analysis. Proteins with HA, Flag, and GFP tags were detected using monoclonal anti-HA (Sangon Biotech), anti-Flag (Beyotime), and anti-GFP (Beyotime) antibodies, respectively.

## GST pull-down assays

Full-length *FT1*, *Gf14b*, *FPL1*, and *FPL7* CDS were amplified and cloned into pGEX-4T-1 or pCold TF DNA (Takara) and then transformed into *Escherichia coli* (Rosetta strain) to express corresponding GST- or His-fused proteins. The purified proteins of the indicated combination were mixed into pull-down buffer containing 50 mM Tris-HCl (pH 7.5), 1 mM EDTA, 150 mM KCl, 1 mM DTT, 5% (*v*/*v*) glycerol, 0.01% (*v*/*v*) Nonidet P-40, and 1 mM phenylmethylsulfonyl fluoride and incubated with glutathione magnetic agarose beads (Sigma) at 4°C for 2 h with gentle shaking. Beads were then washed 4 times and boiled with SDS loading buffer for subsequent immunoblotting analysis. Proteins with GST and His tags were detected using monoclonal anti-GST (Beyotime) and anti-His (Sangon Biotech) antibodies, respectively.

### EMSAs

Full-length *FT1*, *FD1*, *Gf14b*, *FPL1*, *FPL7*, *VRN1*, and *FUL2* CDS were amplified and cloned into pGEX-4T-1, pCold TF DNA, or pMAL-c2X vectors and then transformed into *E. coli* (Rosetta strain) to express corresponding GST-, His-, or MBP-fused proteins. Two to 5 $\mu$g purified proteins were then incubated with biotin 5′-end-labelled DNA probes, for examination of DNA–protein association or protein competition (1×), using an EMSA/Gel-Shift Kit (Beyotime), according to the manual. All primers and probes used are listed in Supplemental Data Set 2.

### ChIP-qPCR assay

ChIP assays were performed using an EpiQuik Plant ChIP Kit following the manual. In brief, leaves of *UBI:VRN1-HA* plants (~3 wks old) were harvested and crosslinked using 1% formaldehyde. After grinding into powder, nuclei were isolated, and chromatin was sonicated to shear the DNA. Sonicated chromatin was immunoprecipitated using IgG or polyclonal anti-HA antibody (Abcam). After incubation, crosslinking was reversed by incubation at 65°C and DNA purified. Enrichment of the *FPL1* and *FPL7* promoter fraction immunoprecipitated by IgG or anti-HA antibody was analyzed by qPCR, using *Actin7* promoter fragments as a negative control. ChIP values were normalized to corresponding input DNA. All primers used in ChIP-qPCR are listed in Supplemental Data Set 2.

### Accession numbers

Sequence data from this article can be found in the Brachypodium Genome Initiative or GenBank databases under the following accession numbers: FPL1, Bradi3g12450; FPL2, Bradi5g04810; FPL3, Bradi2g59820; FPL4, Bradi2g59830; FPL5, Bradi2g09310; FPL6, Bradi2g09320; FPL7, Bradi1g18240; FPL8, Bradi3g21411; FPL9, Bradi1g62652; FT1, Bradi1g48830; VRN1, Bradi1g08340; FD1, Bradi4g36587; and Gf14b, Bradi5g12510.

## Acknowledgments

We sincerely thank Richard M. Amasino for the gift of *phyC* mutants as well as *FT1* and *VRN1* overexpression *B. distachyon* plants.

## Author contributions

L.W. and S.L. designed the experiments. S.L. performed most of the experiments. S.C. and Y.Z. determined the expression patterns of *FPL1* and *FPL7* in different *B. distachyon* tissues. Y.S. did the transcriptome analysis. S.L., Z.Q., and L.W. analyzed the experimental results. S.L. and L.W. wrote the article.

## Supplemental data

The following materials are available in the online version of this article.

**Supplemental Figure S1**. Phylogenetic tree of the FPF1-like family.

**Supplemental Figure S2**. Expression of *FPL1* and *FPL7* is not sensitive to GA treatment.

**Supplemental Figure S3**. Generation of single and double *fpl1* and *fpl7* mutants by CRISPR/Cas9.

**Supplemental Figure S4**. *FPL1* and *FPL7* repress flowering in *B. distachyon*.

**Supplemental Figure S5**. Flowering phenotypes of FPL1 and FPL7 gain- and loss-of-function plants under SD conditions.

**Supplemental Figure S6**. RT-PCR analysis confirming the comparable expression levels of introduced genes in FLCI assays shown in Fig. 2B.

**Supplemental Figure S7**. FLCI and BIFC assays show no interaction signals between FPL1/7 and the control protein.

**Supplemental Figure S8**. Subcellular localization of FPL1/7 and FAC components.

**Supplemental Figure S9**. FPL1 and FPL7 interact with FD1.

**Supplemental Figure 10**. FPL1 and FPL7 interact with Gf14b.

**Supplemental Figure 11**. RT-PCR analysis confirming the comparable expression levels of the introduced genes in LUC activity assays shown in Fig. 3A.

**Supplemental Figure 12**. FPL1 and FPL7 inhibit the interaction between FD1 and Gf14b.

**Supplemental Figure 13**. FPL1 and FPL7 attenuate binding of FD1 and FAC to *cis*-element of the *VRN1* promoter.

**Supplemental Figure 14**. RT-PCR analysis confirming the comparable expression levels of the introduced genes in transactivation assays shown in Fig. 4E.

**Supplemental Figure 15**. Expression of *FPL1*, *FPL7*, *VRN1*, and FAC components in different tissues.

**Supplemental Figure 16**. FT1 and VRN1 form a feedback regulatory loop in *B. distachyon* leaves.

**Supplemental Figure 17**. *VRN1* expression levels in SAMs of *FPL1* and *FPL7* gain- and loss-of-function plants under LDs.

**Supplemental Figure 18**. Generation of *ft1fpl1fpl7* triple mutants by CRISPR/Cas9.

**Supplemental Figure 19**. Flowering phenotype of *ft1* mutants under LDs.

**Supplemental Figure 20**. Representative images of various-aged shoot apices.

**Supplemental Figure 21**. Examination of VRN1 regulation of *FPL7*.

**Supplemental Figure 22**. Examination of FUL2 regulation of *FPL1* and *FPL7*.

**Supplemental Data Set 1**. List of DEGs identified through transcriptomic analysis.

**Supplemental Data Set 2**. Primers and probes used in this study.

**Supplemental Data Set 3**. Statistical data.

**Supplemental File 1**. Text file of the alignment used for phylogenetic analysis in Supplemental Fig. S1.

**Supplemental File 2**. Tree file for phylogenetic analysis in Supplemental Fig. S1.

## Funding

This work was supported by the National Natural Science Foundation of China (32170326, 91640109, 32070339) and

Zhejiang Provincial Natural Science Foundation of China (LZ21C130002, LR21C020002).

*Conflict of interest statement.* None declared.

## References

**Abe M, Kobayashi Y, Yamamoto S, Daimon Y, Yamaguchi A, Ikeda Y, Ichinoki H, Notaguchi M, Goto K, Araki T**. FD, a bZIP protein mediating signals from the floral pathway integrator FT at the shoot apex. Science 2005:**309**(5737):1052–1056. doi:10.1126/science.1115983

**Abelenda JA, Bergonzi S, Oortwijn M, Sonnewald S, Du MR, Visser RGF, Sonnewald U, Bachem CWB**. Source-sink regulation is mediated by interaction of an FT homolog with a SWEET protein in potato. Curr Biol. 2019:**29**(7):1178-+. doi:10.1016/j.cub.2019.02.018

**Alonso-Peral MM, Oliver SN, Casao MC, Greenup AA, Trevaskis B**. The promoter of the cereal VERNALIZATION1 gene is sufficient for transcriptional induction by prolonged cold. PLoS One 2011:**6**(12):e29456. doi:10.1371/journal.pone.0029456

**Alves SC, Worland B, Thole V, Snape JW, Bevan MW, Vain P**. A protocol for Agrobacterium-mediated transformation of Brachypodium distachyon community standard line Bd21. Nat Protoc. 2009:**4**(5):638–649. doi:10.1038/nprot.2009.30

**Chen A, Dubcovsky J**. Wheat TILLING mutants show that the vernalization gene VRN1 down-regulates the flowering repressor VRN2 in leaves but is not essential for flowering. PLoS Genet. 2012:**8**(12):e1003134. doi:10.1371/journal.pgen.1003134

**Collani S, Neumann M, Yant L, Schmid M**. FT modulates genome-wide DNA-binding of the bZIP transcription factor FD. Plant Physiol. 2019:**180**(1):367–380. doi:10.1104/pp.18.01505

**Deng W, Casao MC, Wang P, Sato K, Hayes PM, Finnegan EJ, Trevaskis B**. Direct links between the vernalization response and other key traits of cereal crops. Nat Commun. 2015:**6**(1):5882. doi:10.1038/ncomms6882

**Foster R, Izawa T, Chua NH**. Plant bZIP proteins gather at ACGT elements. FASEB J. 1994:**8**(2):192–200. doi:10.1096/fasebj.8.2.8119490

**Greenup AG, Sasani S, Oliver SN, Talbot MJ, Dennis ES, Hemming MN, Trevaskis B**. ODDSOC2 is a MADS box floral repressor that is down-regulated by vernalization in temperate cereals. Plant Physiol. 2010:**153**(3):1062–1073. doi:10.1104/pp.109.152488

**Guo Y, Wu Q, Xie Z, Yu B, Zeng R, Min Q, Huang J**. OsFPFL4 is involved in the root and flower development by affecting auxin levels and ROS accumulation in rice (*Oryza sativa*). Rice (N Y). 2020:**13**(1):2. doi:10.1186/s12284-019-0364-0

**Hemming MN, Peacock WJ, Dennis ES, Trevaskis B**. Low-temperature and daylength cues are integrated to regulate FLOWERING LOCUS T in barley. Plant Physiol. 2008:**147**(1):355–366. doi:10.1104/pp.108.116418

**Ho WWH, Weigel D**. Structural features determining flower-promoting activity of Arabidopsis FLOWERING LOCUS T. Plant Cell 2014:**26**(2):552–564. doi:10.1105/tpc.113.115220

**Kania T, Russenberger D, Peng S, Apel K, Melzer S**. FPF1 promotes flowering in Arabidopsis. The Plant Cell. 1997:**9**(8):1327–1338. doi:10.1105/tpc.9.8.1327

**Li C, Lin H, Dubcovsky J**. Factorial combinations of protein interactions generate a multiplicity of florigen activation complexes in wheat and barley. The Plant journal: for cell and molecular biology. 2015:**84**(1):70–82. doi:10.1111/tpj.12960

**Li CX, Dubcovsky J**. Wheat FT protein regulates VRN1 transcription through interactions with FDL2. Plant Journal. 2008:**55**(4):543–554. doi:10.1111/j.1365-313X.2008.03526.x

**Liu L, Li C, Teo ZWN, Zhang B, Yu H**. The MCTP-SNARE complex regulates florigen transport in Arabidopsis. Plant Cell 2019:**31**(10):2475–2490. doi:10.1105/tpc.18.00960

**Liu L, Liu C, Hou XL, Xi WY, Shen LS, Tao Z, Wang Y, Yu H**. FTIP1 is an essential regulator required for florigen transport. Plos Biol. 2012:**10**(4):e1001313. doi:10.1371/journal.pbio.1001313

**Melzer S, Kampmann G, Chandler J, Apel K**. FPF1 modulates the competence to owering in Arabidopsis. Plant J. 1999:**18**(4):395–405. doi:10.1046/j.1365-313X.1999.00461.x

**Nagai K, Mori Y, Ishikawa S, Furuta T, Gamuyao R, Niimi Y, Hobo T, Fukuda M, Kojima M, Takebayashi Y, et al.** Antagonistic regulation of the gibberellic acid response during stem growth in rice. Nature 2020:**584**(7819):109–114. doi:10.1038/s41586-020-2501-8

**Nicolas M, Torres-Perez R, Wahl V, Cruz-Oro E, Rodriguez-Buey ML, Zamarreno AM, Martin-Jouve B, Garcia-Mina JM, Oliveros JC, Prat S, et al.** Spatial control of potato tuberization by the TCP transcription factor BRANCHED1b. Nat Plants. 2022:**8**(3):281-+. doi:10.1038/s41477-022-01112-2

**Qin Z, Wu J, Geng S, Feng N, Chen F, Kong X, Song G, Chen K, Li A, Mao L, et al.** Regulation of FT splicing by an endogenous cue in temperate grasses. Nat Commun. 2017:**8**(1):14320. doi:10.1038/ncomms14320

**Qin ZR, Bai YX, Muhammad S, Wu X, Deng PC, Wu JJ, An HL, Wu L**. Divergent roles of FT-like 9 in flowering transition under different day lengths in *Brachypodium distachyon*. Nat Commun. 2019:**10**(1). doi:10.1038/s41467-019-08785-y

**Ream TS, Woods DP, Schwartz CJ, Sanabria CP, Mahoy JA, Walters EM, Kaeppler HF, Amasino RM**. Interaction of photoperiod and vernalization determines flowering time of *Brachypodium distachyon*. Plant Physiol. 2014:**164**(2):694–709. doi:10.1104/pp.113.232678

**Riechmann JL, Meyerowitz EM**. MADS domain proteins in plant development. Biol Chem. 1997:**378**(10):1079–1101.

**Riechmann JL, Wang M, Meyerowitz EM**. DNA-binding properties of Arabidopsis MADS domain homeotic proteins APETALA1, APETALA3, PISTILLATA and AGAMOUS. Nucleic Acids Res. 1996:**24**(16):3134–3141. doi:10.1093/nar/24.16.3134

**Romera-Branchat M, Severing E, Pocard C, Ohr H, Vincent C, Nee G, Martinez-Gallegos R, Jang S, Andres F, Madrigal P, et al.** Functional divergence of the Arabidopsis florigen-interacting bZIP transcription factors FD and FDP. Cell Rep. 2020:**31**(9):107717. doi:10.1016/j.celrep.2020.107717

**Schmid M, Uhlenhaut NH, Godard F, Demar M, Bressan R, Weigel D, Lohmann JU**. Dissection of floral induction pathways using global expression analysis. Development 2003:**130**(24):6001–6012. doi:10.1242/dev.00842

**Smykal P, Gleissner R, Corbesier L, Apel K, Melzer S**. Modulation of flowering responses in different Nicotiana varieties. Plant Mol Biol. 2004:**55**(2):253–262. doi:10.1007/s11103-004-0557-8

**Taoka K, Ohki I, Tsuji H, Furuita K, Hayashi K, Yanase T, Yamaguchi M, Nakashima C, Purwestri YA, Tamaki S, et al.** 14-3-3 proteins act as intracellular receptors for rice Hd3a florigen. Nature 2011:**476**(7360):332–335. doi:10.1038/nature10272

**Wang X, Fan S, Song M, Pang C, Wei H, Yu J, Ma Q, Yu S**. Upland cotton gene GhFPF1 confers promotion of flowering time and shade-avoidance responses in *Arabidopsis thaliana*. PLoS One 2014:**9**(3):e91869. doi:10.1371/journal.pone.0091869

**Wigge PA, Kim MC, Jaeger KE, Busch W, Schmid M, Lohmann JU, Weigel D**. Integration of spatial and temporal information during floral induction in Arabidopsis. Science 2005:**309**(5737):1056–1059. doi:10.1126/science.1114358

**Woods DP, McKeown MA, Dong Y, Preston JC, Amasino RM**. Evolution of VRN2/ghd7-like genes in vernalization-mediated repression of grass flowering. Plant Physiol. 2016:**170**(4):2124–2135. doi:10.1104/pp.15.01279

**Woods DP, Ream TS, Minevich G, Hobert O, Amasino RM**. PHYTOCHROME C is an essential light receptor for photoperiodic flowering in the temperate grass, *Brachypodium distachyon*. Genetics 2014:**198**(1):397–408. doi:10.1534/genetics.114.166785

**Wu L, Liu DF, Wu JJ, Zhang RZ, Qin ZR, Liu DM, Li AL, Fu DL, Zhai WX, Mao L**. Regulation of FLOWERING LOCUS T by a microRNA in *Brachypodium distachyon*. Plant Cell 2013:**25**(11):4363–4377. doi:10.1105/tpc.113.118620

**Zhu Y, Liu L, Shen L, Yu H**. NaKR1 regulates long-distance movement of FLOWERING LOCUS T in Arabidopsis. Nat Plants. 2016:**2**(6):16075. doi:10.1038/nplants.2016.75